Supporting Information

Tunable Thickness and Photoluminescence of Bi-pyramidal Hexagonal β-$NaYF_4$ Microdiscs

Jianle Zhuang,[†] Jing Wang,[†] Xianfeng Yang,[†] Ian D. Williams,[‡] Wei Zhang,[†] Qinyuan Zhang,[§] Zhouming Feng,[§] Zhongmin Yang,[§] Chaolun Liang,[†] Mingmei Wu[†] and Qiang Su[†]*

† MOE Key Laboratory of Bioinorganic and Synthetic Chemistry / State Key Laboratory of Optoelectronic Materials and Technologies, School of Chemistry and Chemical Engineering, Instrumental Analysis and Research Center, Sun Yat-Sen (Zhongshan) University, Guangzhou 510275, P. R. China

‡ Department of Chemistry, Hong Kong University of Science and Technology, Clear Water Bay, Kowloon, Hong Kong, P. R. China

§ MOE Key Laboratory of Specially Functional Materials and Institute of Optical Communication Materials, South China University of Technology, Guangzhou 510640, P. R. China

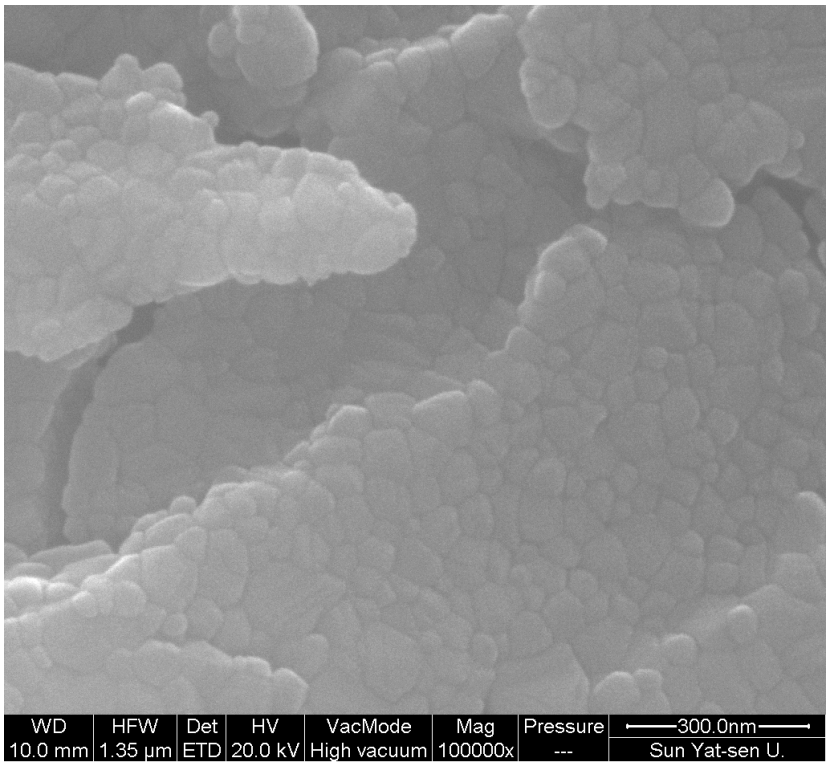

Figure S1. A high magnification SEM image of precursory Y_2O_3 nanoparticles.

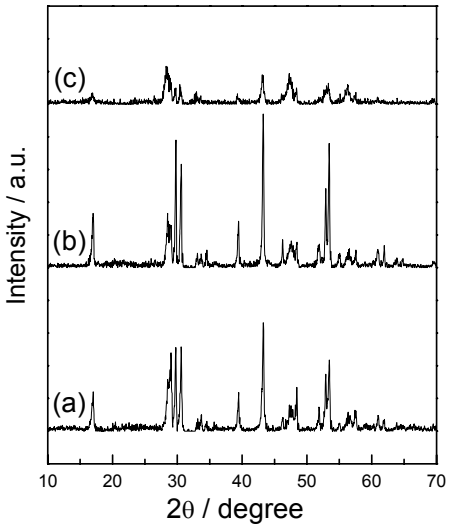

Figure S2. XRD patterns of products synthesized at 220 ^{o}C for 24 h from different solvents. (a) H_2O, (b) acetic acid, and (c) ethylamine.

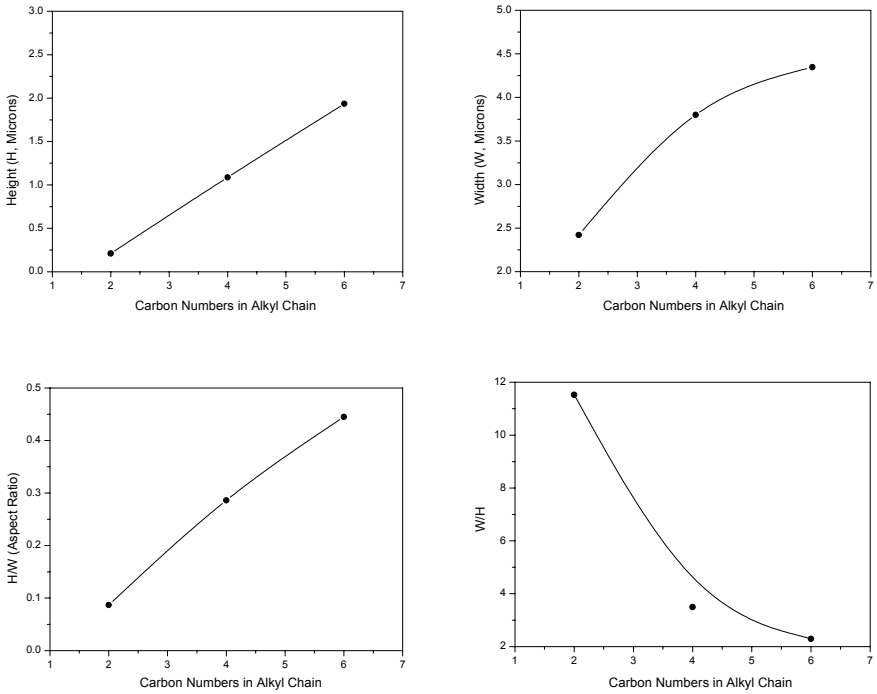

Figure S3. The dependence of disc height (H), width (W) and their ratios (H/W and W/H) on the carbon numbers in alkyl chains of the solvent alcohols.

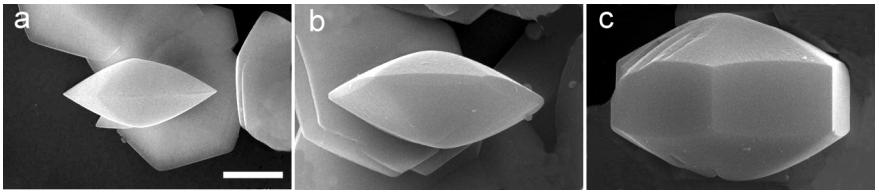

Figure S4. SEM images of three individual β-$NaYF_4$ crystals synthesized at 180 ^oC for 24 h from the three different solvents: (a) ethanol, (b) *n*-butanol, and (c) *n*-hexanol (Scale bar = 1.0 micron).

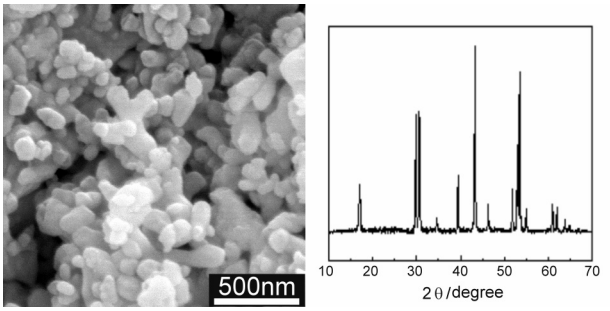

Figure S5. SEM image and powder XRD pattern of β-$NaYF_4$ nanoparticles synthesized at 220 ^oC for 24 h with $Y(NO_3)_3$ as precursor.

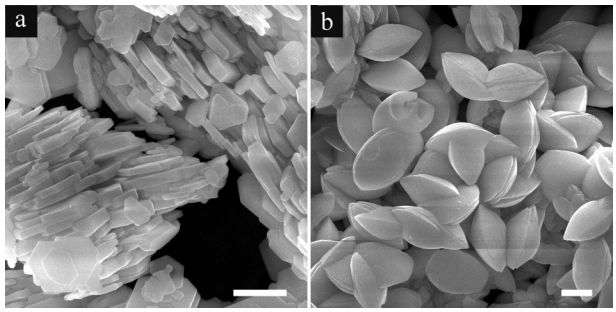

Figure S6. SEM images of the products as mentioned in (a) Figure 5La (i.e. LaF_3) and (b) Figure 5Ho (i.e. $NaHoF_4$). Scale bar = 1.0 micron.

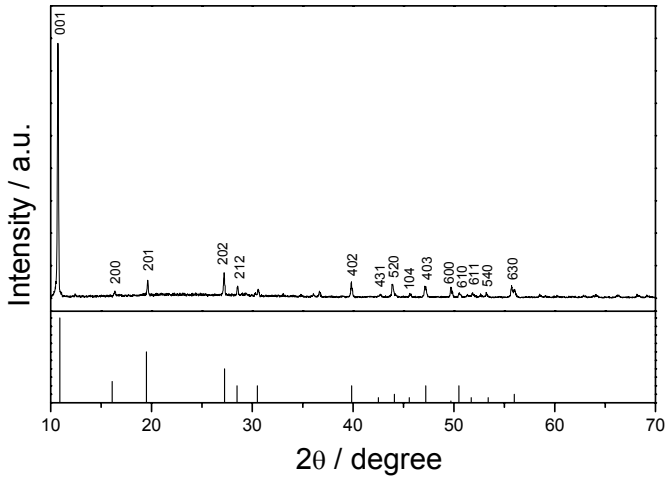

Figure S7. Powder XRD pattern of the product NH_4CeF_5 as shown in Figure 5Ce. This agrees with JCPDS card No. 19-0278.

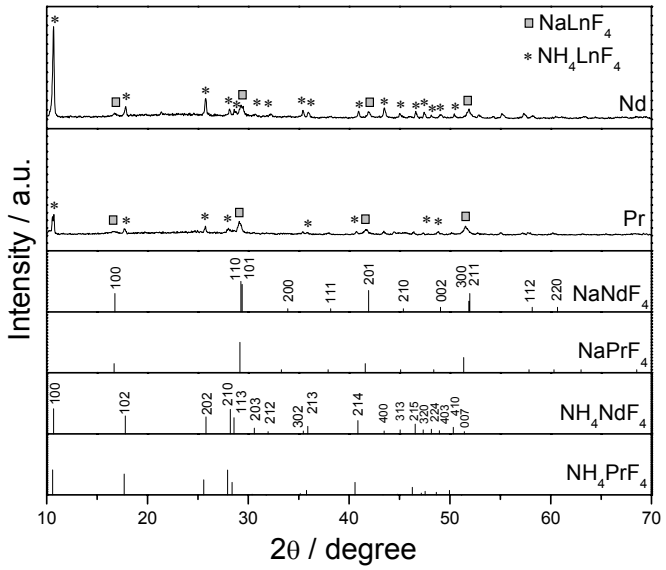

Figure S8. Powder XRD patterns of the products as shown in Figure 5Pr, Nd. They are indexed to be NH_4LnF_4 and β-$NaLnF_4$ respectively according to JCPDS cards No. 43-0828 (0829) and 35-1367. Note: In the JCPDS card of 22-1393, $NaPrF_4$ was indicated to be a cubic phase, in fact, it is an iso-structure to β-$NaNdF_4$ JCPDS card No. 35-1367. The peak at 2θ/29.1^o is composed of two overlapping diffraction peaks indexed as 110 and 101.

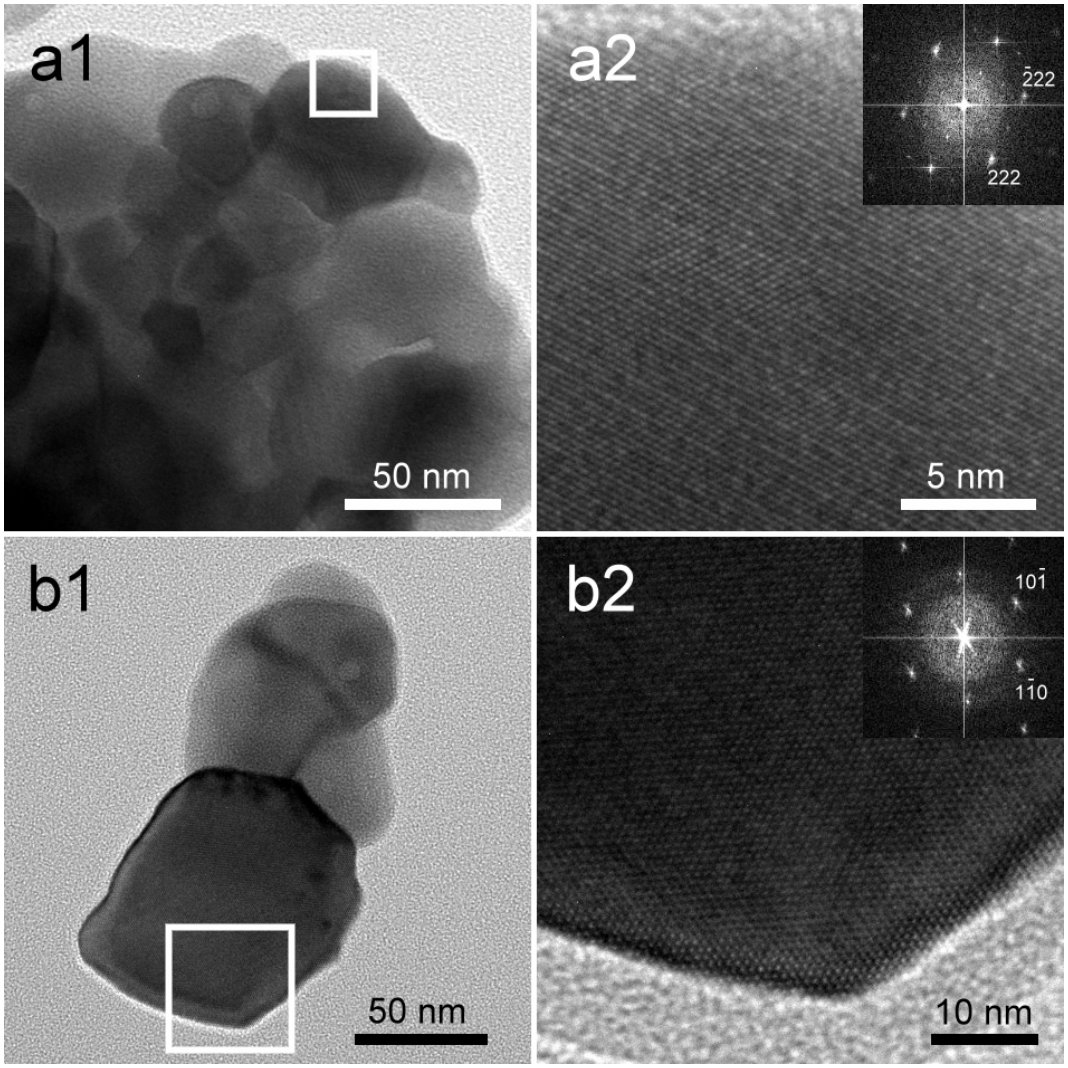

Figure S9. (a1) TEM image of an aggregate of Y_2O_3 nanocrystals, (a2) HRTEM image from one typical larger crystal with the zone axis of $[0\,\bar{1}\,1]$ as confirmed by the FFT in the inset; (b1) TEM image of another aggregate of Y_2O_3 nanocrystals, (b2) HRTEM image from the solid-line enclosed square in (b1) with the zone axis of [111] as confirmed by the FFT in the inset. These images strongly suggested the highly single crystalline quality of the Y_2O_3 precursor.

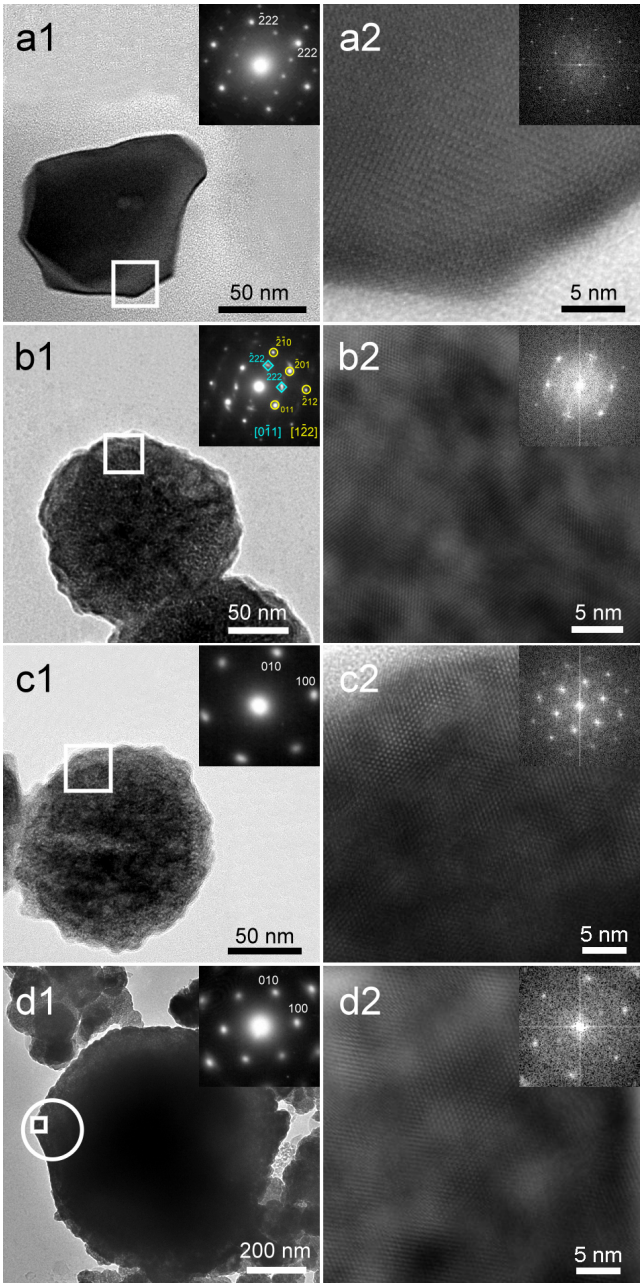

Figure S10. Corresponding to Figure 6 with an addition of HRTEM images and related FFT patterns. (a1-d1) TEM images and related SAED patterns (inserts) and (a2-d2) HRTEM image from respective solid-line-enclosed squares in (a1-d1) and related FFT patterns (inserts) of (a) precursory Y_2O_3, (b-d) some individual grains in the product as shown in Figure 1b (i.e. Figure 2b). (b) Single crystal-like grain with nanopores is a mixture phase of Y_2O_3 and β-$NaYF_4$, the blue and yellow spots in the insert of (b1) are corresponding to Y_2O_3 and β-$NaYF_4$ with zone axes of $[0\bar{1}1]$ and $[1\bar{2}2]$ respectively. (c) Single crystal-like grain with nanopores consists of pure phase of β-$NaYF_4$. (d) The hexagonal disc-like grain without pores is a phase pure β-$NaYF_4$ crystal. The same zone axis in (c) and (d) is along the [001] direction, i.e. *c*-axis.

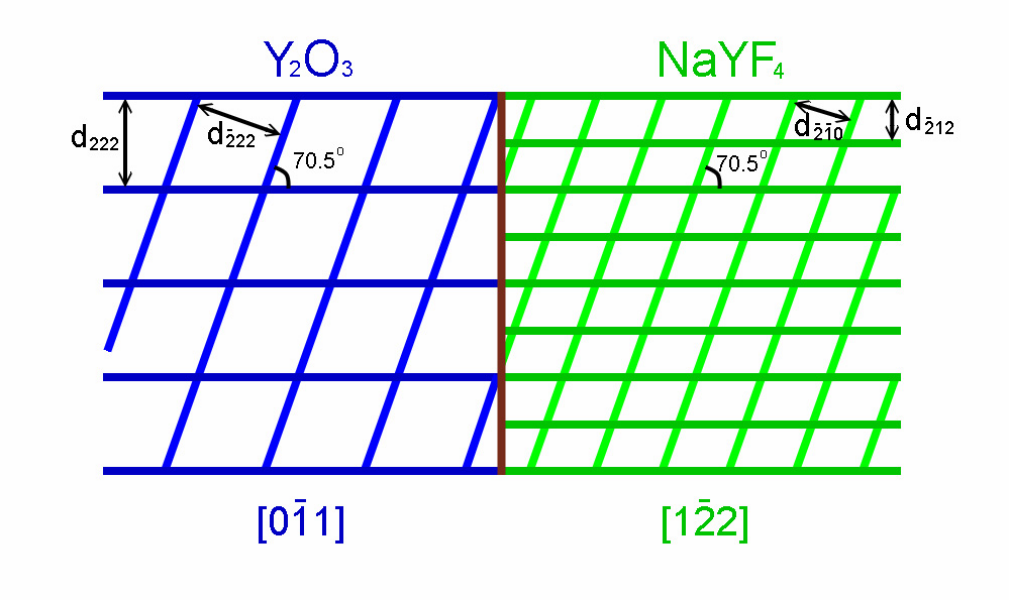

Figure S11. The schematic relationship of d-spacings and the orientations between $(222)_{YO}$ and $(\bar{2}12)_{NYF}$ as well as $(\bar{2}22)_{YO}$ and $(\bar{2}\bar{1}0)_{NYF}$ planes, respectively. The d-spacings have such a relationship: $d_{222(YO)} \sim d_{\bar{2}22(YO)} \sim 2d_{\bar{2}12(NYF)} \sim 1.5d_{\bar{2}\bar{1}0\ (NYF)}$. According to Figure 6b and Figure S10b, the lattice planes $(222)_{YO}//(\bar{2}12)_{NYF}$ and $(\bar{2}22)_{YO}//(\bar{2}\bar{1}0)_{NYF}$. The zone axes $[0\bar{1}1]_{YO}//[1\bar{2}2]_{NYF}$.

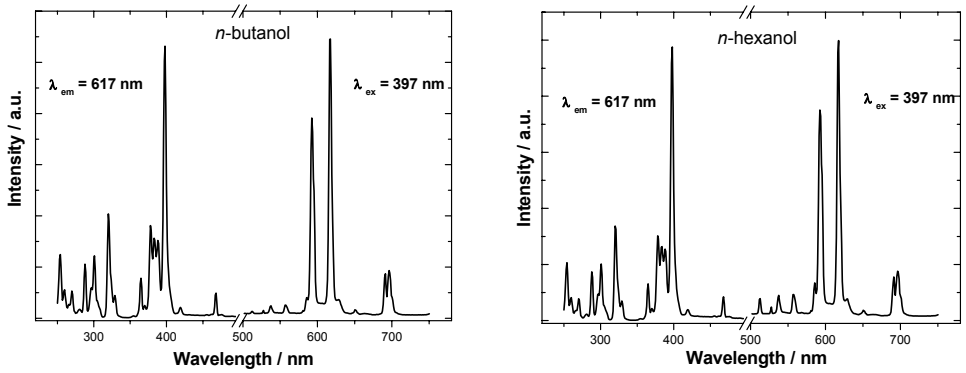

Figure S12. Excitation (λ_{em}= 617 nm) and emission (λ_{ex} = 397 nm) spectra of β-$NaYF_4$: $0.05Eu^{3+}$ synthesized in *n*-butanol and *n*-hexanol, respectively.

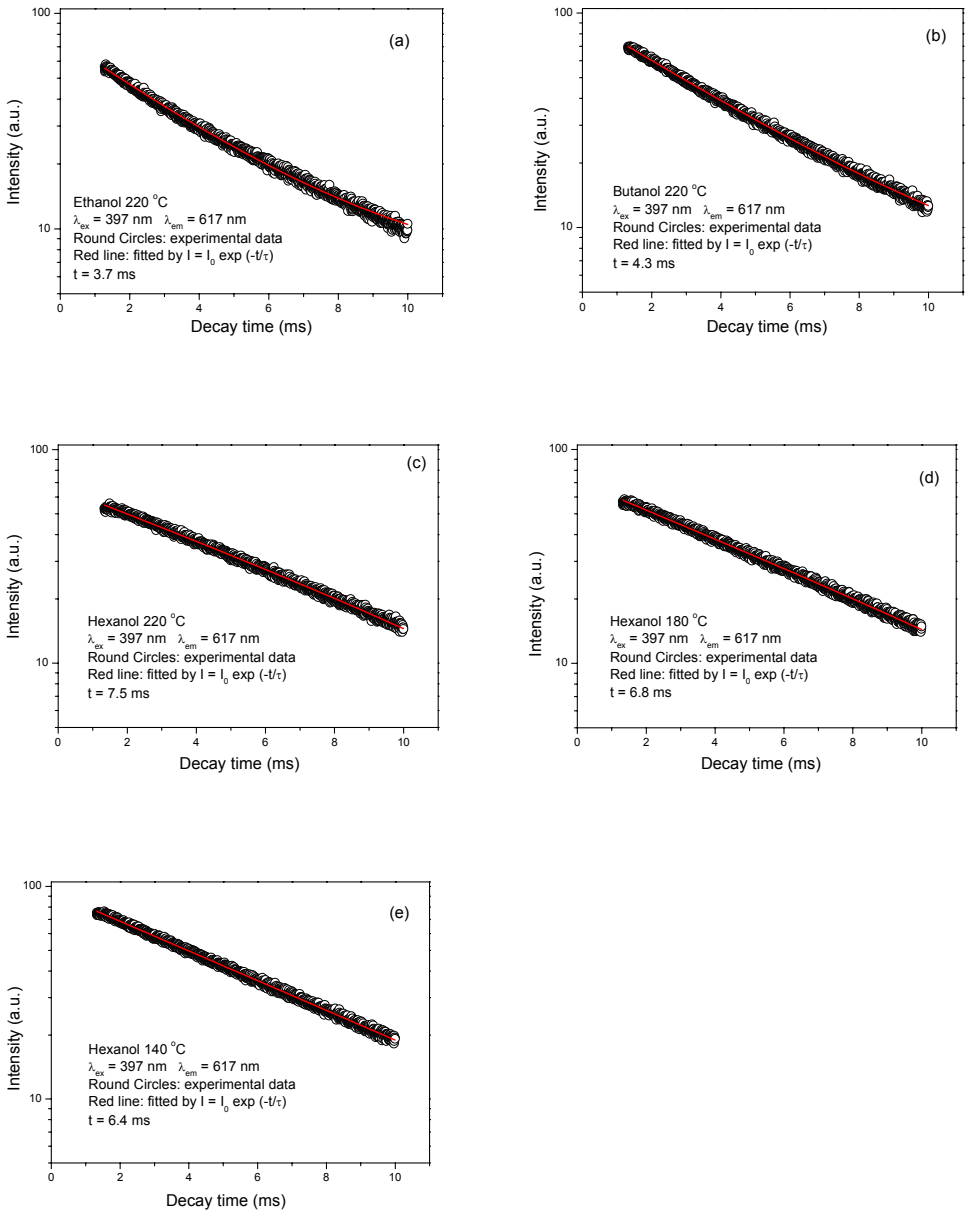

Figure S13. The decay curves of Eu^{3+} doped β-$NaYF_4$ samples upon excitation at 397 nm. The samples (a), (b) and (c) grown at 220 °C in ethanol, *n*-butanol and *n*-hexanol, respectively. The samples (d) and (e) grown in hexanol at 180 °C and 140 °C respectively.

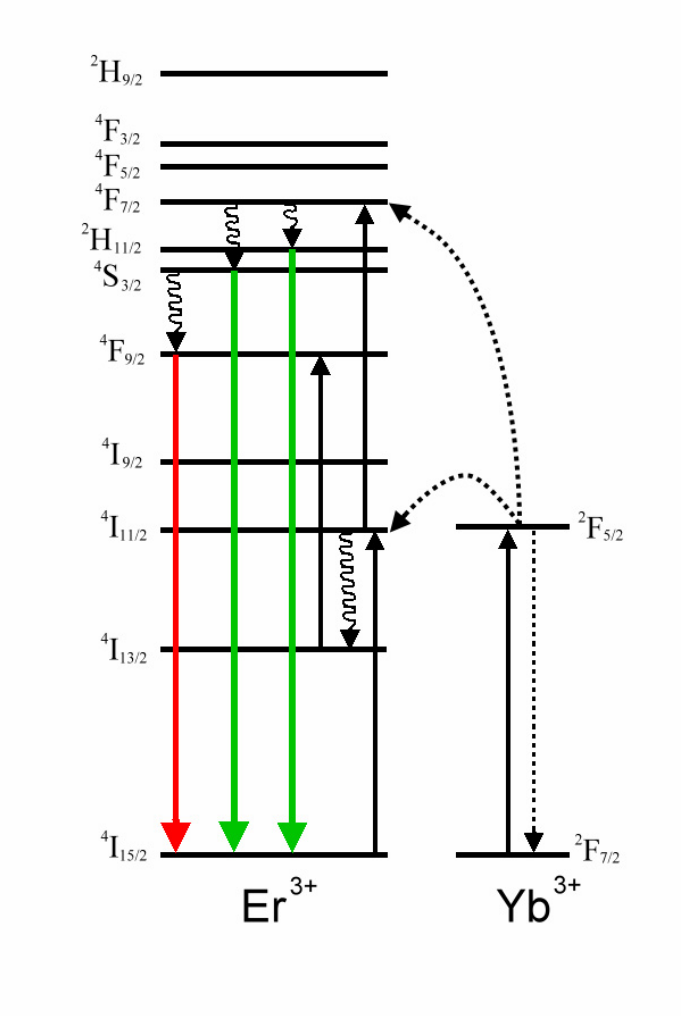

Figure S14. Schematic illustration of the Up-conversion process of Er^{3+} with Yb^{3+} as the promoter for β-$NaYF_4$: Yb^{3+}/Er^{3+} crystals.